ELSEVIER

Journal of Chromatography A, 868 (2000) 217–227

JOURNAL OF CHROMATOGRAPHY A

www.elsevier.com/locate/chroma

Different elution modes and field programming in gravitational field-flow fractionation
2. Experimental verification of the range of conditions for flow-rate and carrier liquid density programming

Jana Plocková*, Josef Chmelík

Institute of Analytical Chemistry, AS CR, 611 42 Brno, Czech Republic

Received 24 August 1999; received in revised form 19 November 1999; accepted 19 November 1999

Abstract

Gravitational field-flow fractionation utilises the Earth's gravitational field as an external force that causes the settlement of particles towards the channel accumulation wall. Hydrodynamic lift forces oppose this action by elevating of particles from the channel accumulation wall. Therefore there are several possibilities to modulate the resulting force field acting on particles in gravitational field-flow fractionation. Regarding the force field programming in gravitational field-flow fractionation, this work focused on two topics: changes of the difference between particle density and carrier liquid density in Brownian and focusing elution modes and influencing of lift forces achieved by changing the flow-rate in focusing elution mode. We have found and described the experimental conditions applicable to force field programming in the case of separations of silica gel particles by gravitational field-flow fractionation. It was shown that the effect of carrier liquid viscosity in the water–methanol system is implemented as an additional factor enhancing the desired effect of carrier liquid density. Some other forces influencing the retention behaviour of the model particles are discussed.

Keywords: Gravitational field-flow fractionation; Field-flow fractionation; Field programming; Density; Viscosity; Hydrodynamic lift forces; Electrostatic repulsion

1. Introduction

Gravitational field-flow fractionation (GFFF), the experimentally simplest field-flow fractionation (FFF) technique, is an inexpensive tool for a successful separation, characterisation and micropreparation of various particles [1–6], polymer latexes [7,8], glass beads [9], and cells [10–12]. Nevertheless, the implementation of GFFF for a wide variety of analytes requires one to broaden the separation capabilities of this technique.

The separation effect in FFF is reached by combined action of a non-uniform flow velocity profile of a carrier liquid and a transverse force field applied. The force field can be programmed to obtain optimised separations in terms of time and res-

*Corresponding author.

0021-9673/00/$ – see front matter
PII: S0021-9673(99)01235-2

olution. Giddings and co-workers [13,14] described the control of retention in sedimentation FFF through field strength programming by changes in rotation speed and through carrier liquid density programming.

Because GFFF utilises the Earth's gravitational field as an external force which causes the settlement of particles towards the channel accumulation wall, it was thought that the force field in GFFF cannot be changed. However, there are several possibilities to control the resulting force field acting on particles [15]. Based on the equations describing the concentration profiles of analytes and their dependence on the elution mode mechanisms, it was suggested that the resulting force field can be changed by varying the angle between the Earth's gravitational field and the longitudinal axis of the channel, or by the use of carrier liquids having different densities, in Brownian elution mode. Furthermore, in focusing elution mode, it can be also modulated by changing the flow-rate [15]. Several previously reported works on GFFF support this theoretical conclusions. Giddings et al. [1] found that the retention ratio of silica gel particles is dependent on both: flow-rate and carrier liquid (0.01 *M* ammonia, methanol and isobutanol were tested). The effect of flow-rate on the retention of silica gel particles was studied by Pazourek and co-workers [2,3]. The separation of particles or cells resulting from their different densities have been reported as well (separations of microporous silica and polystyrene latex particles [16], zeolite particles [17] and red blood cells [9]).

Regarding the programming of the resulting force acting on particles in GFFF, this paper is focused on two factors: (1) changes of the difference between particle density and carrier liquid density and (2) influence of lift forces controlled by modulating the flow-rate.

The other possibilities mentioned in Ref. [15] are not discussed in this paper.

The aim of this work is to demonstrate that the phenomena considered in the previous work [15] are occurring in the predicted way. Furthermore, we want to broaden and systematise the experimental data and to find a properly functioning range of flow-rates and carrier liquid densities for the optimisation of force field programming in GFFF.

2. Experimental

2.1. Equipment and materials

The experimental arrangement has been described elsewhere [2,6,23]. The separation channels were cut in spacers of height 80 or 150 μm. The spacer was then sandwiched between two float glass plates and the latter were clamped together with two Plexiglas bars. Three channels were used in this work. The width of all the channels was 2 cm. The height (further denoted w) and the length (further denoted L) of the channels were as follows: channel I, $w=80$ μm, $L=35$ cm; channel II, $w=150$ μm, $L=35$ cm; channel III, $w=150$ μm, $L=30$ cm. Because of the tapered inlet and outlet ends, the geometrical void volumes were as follows: channel I, 0.51 ml; channel II, 0.96 ml; and channel III, 0.81 ml. The fractionations were performed with an HPP 4001 high-pressure pump (Laboratory Instruments, Prague, Czech Republic). An UVM 4 spectrophotometric detector (Development Workshops AS CR, Prague, Czech Republic), equipped with a Z-shaped cell with an optical path of 5 mm, operated at 254 nm.

The samples were non-porous silica gel particles of diameter 0.63 and 1.6 μm (a gift from E. Kováts, SFIT, Lausanne, Switzerland) and porous silica gel particles Sepharon SGX, here denoted according to their nominal diameters 5 and 10 μm (Tessek, Prague, Czech Republic). The carrier liquids were Milli-Q water, methanol analytical-reagent grade (Merci, Czech Republic) and their mixtures. The densities of 0.997 and 0.787 g/cm^3 (at 25°C) for water and methanol, respectively, were used for calculations. All experiments were performed at 25°C.

2.2. Procedure

For the sample preparation, the analyte was suspended in a desired volume of the carrier liquid and sonicated for 10 min. In the case of the porous particles, sonication in the detergent solution was proved to be an adequate as the sample preparation procedure [18]. However, in pure water the situation could be different. Hence, we followed the ultrasound stirring by boiling for 3 min in order to avoid

Table 1
The comparison between the theoretical values of retention ratio (R_{theor}) and the experimentally obtained values of retention ratio (R_{exp}) including standard deviations for the 0.63-μm particles, the channel height $w=150$ μm and two carrier liquids

Retention values	Methanol	Water
R_{theor}	0.100	0.115
R_{exp} at the flow-rate 0.67 cm/min	0.150±0.006	0.181±0.003
R_{exp} at the flow-rate 6.67 cm/min	0.155±0.004	0.192±0.007
R_{exp} at the flow-rate 66.67 cm/min	0.161±0.006	0.198±0.014
$R_{exp}-R_{theor}$ at the flow-rate 0.67 cm/min	0.050	0.066
$R_{exp}-R_{theor}$ at the flow-rate 6.67 cm/min	0.055	0.077
$R_{exp}-R_{theor}$ at the flow-rate 66.67 cm/min	0.061	0.083

gas and thoroughly wet all the particle cavities (the cavities influence the apparent density of the particle). Before each injection, ultrasound stirring of the sample for 2 min was repeated. After injection performed with a long-needle syringe through a septum into the channel inlet, the particles were allowed to settle for the stop-flow time calculated for each particular analyte and carrier liquid, as described elsewhere [1,2] (for non-porous and porous particles $\Delta\rho=1.2$ and 0.5 g/cm^3, respectively). Then the flow was switched on and the sample was eluted through the channel to the detector.

For calculations of the retention ratio (R), a dead volume (V_0) of each particular analysis was taken from its fractogram. Thus obtained values of V_0 were in a good accordance (deviations within 4%) with V_0 obtained as an average elution volume of benzoic acid (five measurements for each particular flow-rate). The values of R reported in this work are averages of five adequate measurements with a relative standard deviation bellow 2% for the most experiments and never above 5%. The standard deviations are shown in Tables 1–3.

Table 3
The comparison between the theoretical values of retention ratio (R_{theor}) and the experimentally obtained values of retention ratio (R_{exp}) including standard deviations for the 1.6-, 5- and 10-μm particles, the channel height 150 μm, the linear flow-rate 33.33 cm/min and water as carrier liquid

Retention values	1.6-μm	5-μm	10-μm
R_{exp}	0.085±0.001	0.187±0.008	0.288±0.002
R_{theor}	0.031	0.098	0.193
$R_{exp}-R_{theor}$	0.054	0.089	0.095

3. Results

3.1. Brownian elution mode

The retention ratio in FFF is defined as a ratio of

Table 2
The comparison between the theoretical values of retention ratio (R_{theor}) and the experimentally obtained values of retention ratio (R_{exp}) including standard deviations (SDs) for the 1.6-, 5- and 10-μm particles, the channel height 80 μm, the linear flow-rate 31.25 cm/min and two carrier liquids

Retention values	1.6-μm		5-μm		10-μm	
	Methanol	Water	Methanol	Water	Methanol	Water
R_{exp}	0.117	0.191	0.229	0.346	0.295	0.510
SD	±0.002	±0.008	±0.002	±0.008	±0.050	±0.010
R_{theor}	0.057	0.066	0.182	0.181	0.352	0.352
$R_{exp}-R_{theor}$	0.060	0.125	0.047	0.165	−0.057	0.158

the elution volume of non-retained substance and the elution volume of a retained analyte; $R=V_0/V_e$. In Brownian elution mode, the retention ratio R depends on two main factors: the strength of the field applied (in the case of GFFF, it is constant and characterised by $1G$) and the properties of analytes. For this purpose, the properties of analytes can be described by two parameters: analyte–field interaction parameter and diffusion coefficient [19].

In GFFF, the analyte–field interaction parameter is the effective mass of the particle: $m_{ef}=V_p(\rho_p-\rho_{cl})$, where V_p is the volume of the particle, ρ_p and ρ_{cl} are densities of the particle and of the carrier liquid, respectively. This parameter, if coupled with the field, refers to transport of analyte towards the channel accumulation wall and formation of a concentration gradient. It means that any change in carrier liquid density results in a change of the analyte–field interaction parameter m_{ef}. Diffusion coefficient describes the Brownian motion of an analyte and refers to the decrease of the concentration gradient, hence, to the transport of an analyte away from the accumulation wall.

For an expression of the dependence of R on the density of carrier liquid in the ideal case of Brownian elution mode (provided that $R\leq 0.2$) [20] we used the simplified Eq. (1)

$$R=\frac{36kT}{(\rho_p-\rho_{cl})\pi d^3 Gw} \quad (1)$$

where k is the Boltzmann constant, T is the temperature, d is the particle diameter and G is the gravitational constant.

According to Eq. (1), decreased density of the carrier liquid results in a lower retention ratio. This assumption is verified experimentally for the 0.63-μm nonporous silica particles, see the fractograms in Fig. 1, revealing the shift of the particle peak, when water is substituted by methanol. The flow-rate dependence of the retention ratios at two different carrier liquid densities, is shown in Fig. 2. It is obvious that the decreased density of the carrier liquid, when water is substituted by methanol, resulted in essentially lower retention ratios at all measured flow-rates for both channel heights. It offers the possibility to employ carrier liquid density gradients for optimised separations. Curves B, C, D expectedly do not show any apparent dependence of R on the flow-rate. Curve A reveals a significant dependence of R on the flow-rate and will be discussed below.

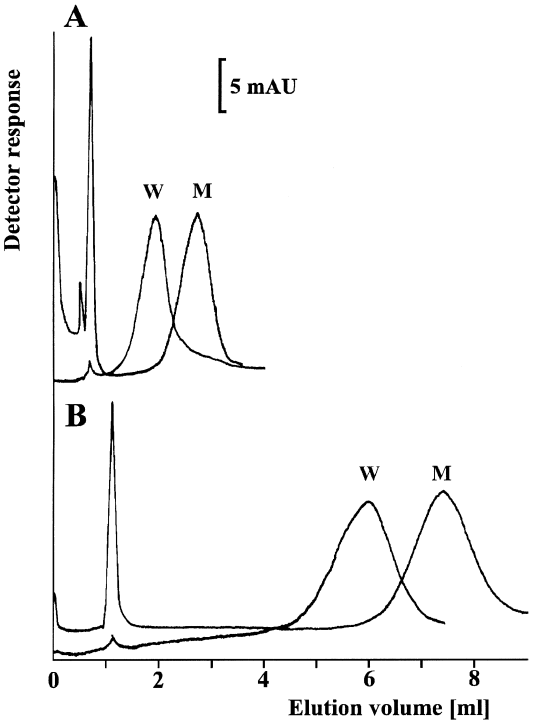

Fig. 1. The dependence of elution volume of 0.63-μm nonporous silica gel particles on density of carrier liquid in Brownian elution mode. Water (W) and methanol (M) were used as carrier liquids. A 2-μl aliquot of a suspension (2 mg/ml) was injected and run at a flow-rate of 0.1 ml/min. Fractograms A hold for the channel height $w=80$ μm, fractograms B for $w=150$ μm.

3.2. Steric elution mode

In the steric elution mode, the retention ratio depends only on the diameter of an analyte ($R=3d/w$). As R depends neither on the carrier liquid density, nor on the flow-rate (provided that the requirement of steric elution mode is fulfilled), no gradient elution can be applied, therefore this elution mode is not discussed in this work.

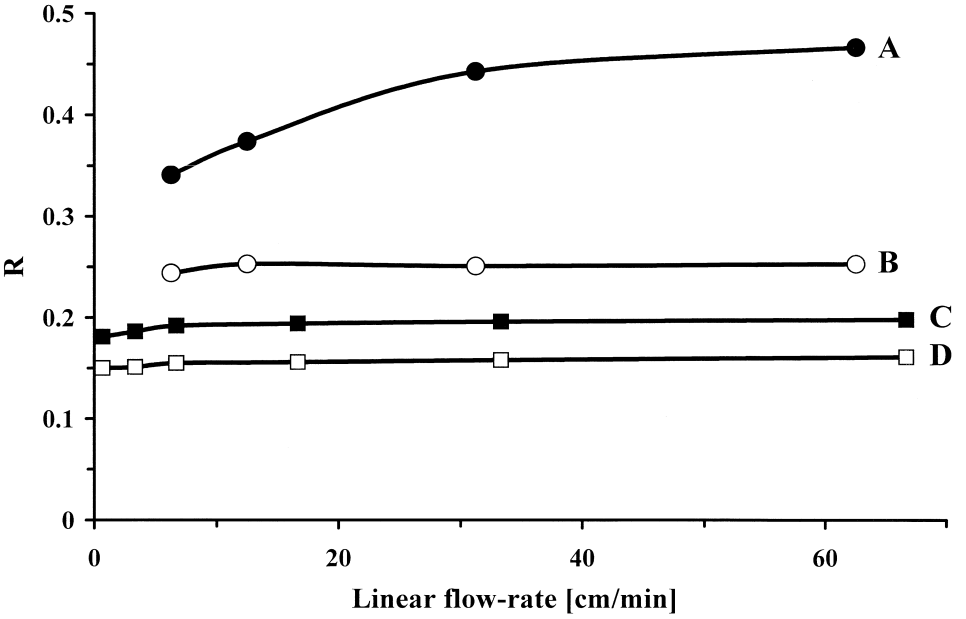

Fig. 2. The dependence of retention ratio R of 0.63-μm nonporous silica gel particles on linear flow-rate. The comparison between two carrier liquid densities and two channel heights. The concentration of the particles in the model suspension was 2 mg/ml, the injected volume was 2 μl. The curves A and B refer to the water and methanol, respectively, at the channel height 80 μm (circles). The curves C and D refer to water and methanol, respectively, at the channel height 150 μm (squares).

3.3. Focusing elution mode

At least two counteracting forces are necessary for the formation of the focused zone of an analyte. The distance of the centre of the focused zone (i.e., the position, where the resulting force acting on the analyte equals zero) from the channel bottom is denoted s. The retention ratio can be expressed in the form $R=6s/w$. In the focusing elution mode in GFFF, the counteracting forces are the gravitational force and the hydrodynamic lift force [22]. The analyte zones are then located in the flow velocity profile at those positions, where the effective particle weight equals the lift force. It follows that any change in these counteracting forces results in the change of the distance s and thus in the change of R.

The effective particle weight $[F_G=Gm_{ef}=GV_p(\rho_p-G_d)]$ can be influenced by using carrier liquids having different densities (G_d). The hydrodynamic lift forces can be modulated as well, as it can be seen from the next equations.

The magnitude of the inertial lift force (when the particle is relatively far away from the channel wall) could be calculated according to Eq. (2) [32].

$$F_I = -\frac{81}{4}\pi\rho_{cl}u^2\frac{r^4}{w^2}(1-2\delta)\frac{K^2-(1-2\delta)^2}{1-K^2} \qquad (2)$$

where F_I is the inertial lift force, u is the average linear velocity of the carrier liquid, r is the particle radius, δ is the dimensionless distance of the particle centre from the channel bottom ($\delta=x/w$, where x is the absolute distance) and $K=0.62$. This equation does not include the influence of viscosity and does not describe thoroughly the behaviour of particles in the close vicinity to the channel wall.

For the near-wall lift force (i.e., the force of non-inertial origin acting additionally on particles in the region very near to the wall), an empirically obtained Eq. (3), which includes the observed influence of viscosity, was suggested, [33]

$$F_{NW} = 6C\eta u\frac{r^3}{hw} \qquad (3)$$

where F_{NW} is the near-wall lift force, C is an empirical constant, η is the dynamic viscosity of the carrier liquid, and h is the closest distance between the particle surface and the channel bottom.

It is shown that the magnitude of lift forces increases with increasing flow-rate, with decreasing channel height, with increasing particle radius, the increasing viscosity of the carrier liquid and depends dramatically on the position in the channel height cross-section. It follows, that we can influence the hydrodynamic lift forces by changes in flow-rate, accomplished by programmed pumping, by channels with non-constant cross-sections [15] or by viscosity changes.

The fractograms in Fig. 3 illustrate the dependence of a resulting force field on the density of the used carrier liquid for focusing elution mode. It is apparent for all the measured analytes that the decreased carrier liquid density, when water is substituted by methanol, resulted in a lower value of R.

The fractograms in Fig. 4 show that even smaller carrier liquid density differences resulted in obvious shifts of the particle peaks. The differences of retention in different water–methanol mixtures were pronounced most significantly for the 1.6-μm particles. These results showed that within the range of R in water and in methanol, any desired R can be obtained by the use of a proper water–methanol mixture. This enables the functioning of carrier liquid density gradients.

The influence of both carrier liquid density and flow-rate on retention of the particles at the channel height 80 μm is demonstrated in Fig. 5, where the values R obtained in the two carrier liquids are plotted against linear flow-rate. It is apparent that R of any particle at any flow-rate in methanol as carrier liquid is lower than that in water. Furthermore, all the curves plotted in Fig. 5 show the expected increase of R with the increasing flow-rate. The dependence of R on the flow-rate for two channel heights and water as a carrier is documented in Fig. 6. The measurements reported in Figs. 5 and 6 define conditions for functioning of the considered flow-rate gradients. Furthermore, the comparison between the curves A and C, B and D or E and F in Fig. 6 indicates that considered amplifying of the hydro-

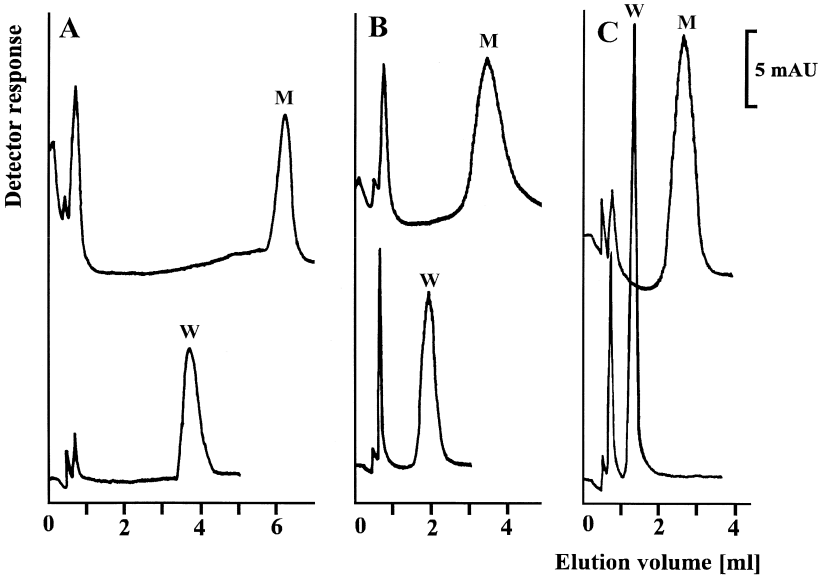

Fig. 3. The dependence of elution volume of the model silica gel particles on density of carrier liquid at the channel height $w=80$ μm. Water (W) and methanol (M) were used as carrier liquids. The concentrations of the particles in the model suspensions were as follows: the nonporous 1.6-μm particles (fractograms A) were 2 mg/ml, the porous 5-μm particles (fractograms B) were 2 mg/ml, and the porous 10-μm particles (fractograms C) were 8 mg/ml. Aliquots (8 μl) of the suspensions were injected and run at a flow-rate of 0.5 ml/min.

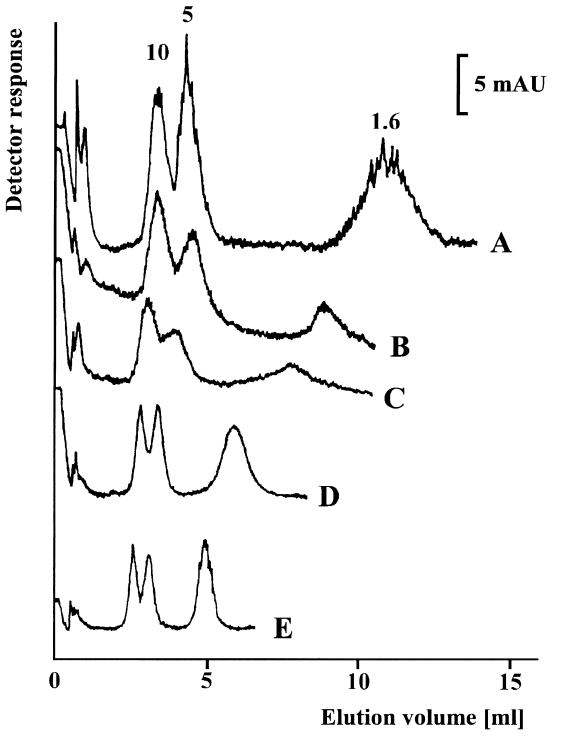

Fig. 4. The dependence of elution volume of the model silica gel particles on density of carrier liquid at the channel height 150 μm. Fractogram A refers to 100% methanol, B refers to 86% (v/v) methanol in water, C refers to 67% methanol in water, D to 50% methanol in water and fractogram E refers to pure water. Nonporous 1.6-μm silica gel particles and porous 5-μm and 10-μm particles were used as model analytes. A 6-μl aliquot of the model particle mixture was injected and run at a flow-rate of 1 ml/min.

dynamic lift-force gradient in channels with decreasing channel heights by the effect of $1/w^2$ [15] is possible.

4. Discussion

4.1. Brownian elution mode

The resulting force field acting on particles can be modulated by changing the density of the carrier liquid used. Curves B, C, D in Fig. 2 show that the 0.63-μm nonporous silica gel particles elute in Brownian elution mode under these conditions (for $w=150$ μm in both methanol and water as carrier liquids and for $w=80$ μm in methanol as carrier liquid). Steric elution mode can be excluded because the retention ratio is higher than $3d/w$, and simple focusing elution mode induced dominantly by hydrodynamic lift forces can be excluded because R does not depend significantly on flow-rate.

On contrary, curve A in Fig. 2 evidences that at $w=80$ μm, hydrodynamic lift forces act on 0.63-μm particles in water. It is apparent that these forces act stronger in water than in methanol (compare curves A and B in Fig. 2). These two carrier liquids differ not only in density but in viscosity as well (the viscosity of methanol and water at 20°C is 0.55 and 1.00 cP, respectively). It seems that the viscosity difference, when methanol is replaced by water (under the same experimental conditions), is responsible for such a different action of the hydrodynamic lift forces and advantageously amplifies the effect of density difference on retention ratio. This offers an additional source for carrier liquid gradients: a viscosity gradient, however, not in Brownian elution mode but in the focusing one. To specify the influence of viscosity, some other experiments are investigated as an ongoing project.

For detailed evaluation of retention behaviour of the 0.63-μm nonporous silica particles we used the extended Eq. (4) covering both Brownian and steric elution mode [21].

$$R_{\text{theor}} = 6(\alpha - \alpha^2) + 6\lambda(1-2\alpha)\left[\coth\left(\frac{1-2\alpha}{2\lambda}\right) - \frac{2\lambda}{1-2\alpha}\right] \quad (4)$$

where $\alpha = d/2w$, $\lambda = 6kT/[(\rho_p - G_d)\pi d^3 G w] = l/w$ and $l = D/|W|$, l is the mean layer thickness of the analyte zone.

By substitution of 2.2 g/cm^3 for the particle density (ρ_p) and 0.63 μm for the particle diameter (d) in Eq. (4) we obtained the theoretical values of the retention ratio R_{theor} (see Table 1). It should be emphasised that the apparently very small difference between R_{theor} in methanol and R_{theor} in water at $w=150$ μm means a significant difference between the corresponding theoretical elution volumes V_{theor}. The V_{theor} values are 12.0 and 10.4 ml in methanol and water, respectively. The comparison between the

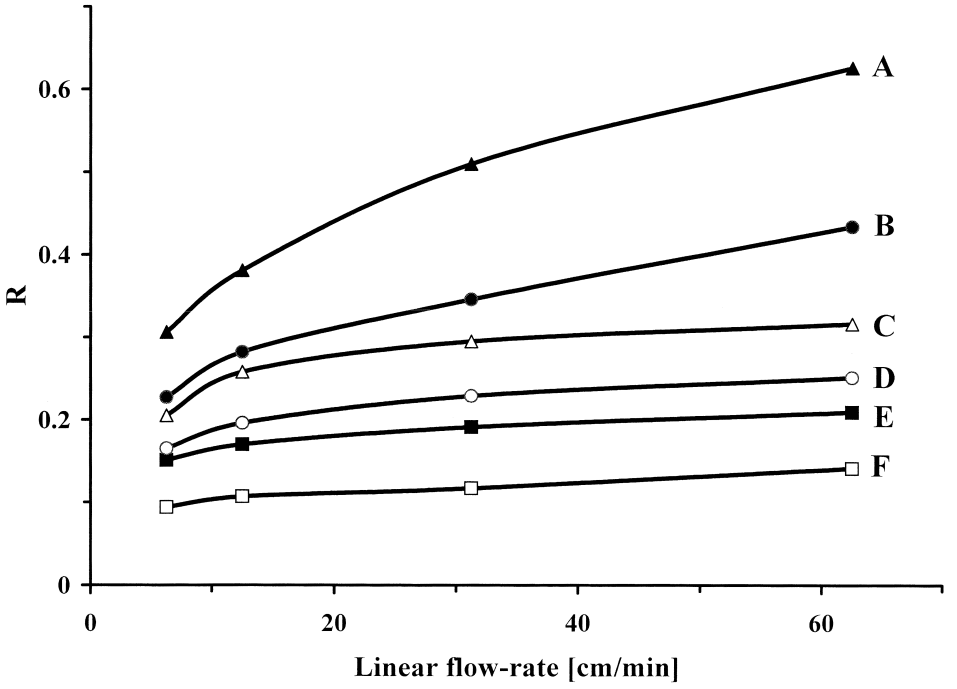

Fig. 5. The dependence of retention ratio R of the model silica gel particles on the linear flow-rate for two carrier liquids of different densities at the channel height 80 μm. The triangles denote 10-μm particles, the circles denote 5-μm particles, and the squares denote 1.6-μm particles. The full signs denote measurements in water as carrier liquid and the empty signs refer to methanol as carrier liquid. Curve A holds for 10-μm particles and water as carrier liquid, B holds for 5-μm particles and water, C for 10-μm particles and methanol, D for 5-μm particles and methanol, E for 1.6-μm particles and water, F for 1.6-μm particles and methanol. The concentrations of particles in the model suspensions were 2 mg/ml and 8-μl volumes were injected.

experimentally obtained values of retention ratio R_{exp} and the values R_{theor} calculated according to Eq. (4) (see Table 1) suggests that in all the measurements reported in Fig. 2, some forces acted on particles in the opposite direction to the gravity. We suppose that besides hydrodynamic forces the electrostatic repulsion could be responsible for the observed difference $R_{exp}-R_{theor}$.

The action of hydrodynamic lift forces is evident from flow-rate dependence. Curve A in Fig. 2. indicates that in the channel of $w=80$ μm, hydrodynamic lift forces dominate, which complicates any quantitative considerations on the proportional contributions of other implemented forces. Hydrodynamic lift forces act more strongly in thinner channels, where the particle diameter reaches approximately 1% of the channel height.

In order to evaluate the proportional responsibility of lift forces for the difference $R_{exp}-R_{theor}$, the experimental results obtained in the thicker channel ($w=150$ μm) were used, where the hydrodynamic lift forces are weaker (see Eq. (2)). The evaluation was carried out by comparison between the contributions of hydrodynamic and some other forces. The increase in R, when the flow-rate of water increased 100-times (from a very low flow-rate of 0.67 cm/min to a relatively high one of 66.67 cm/min), was 0.017, which is 25.8% of the difference $R_{exp}-R_{theor}$ (see Table 1). It can be concluded that lift forces participate to a relatively low extent compared to other forces, which contribute by 74.2%. We assume, that the forces contributing prevalently to the deviations from R_{theor} in this case, are electrostatic repulsive forces. The role of the electrostatic repulsive forces in water has previously been proved experimentally by varying an ionic strength of the carrier liquid [3].

The increase in R, when the flow-rate of methanol

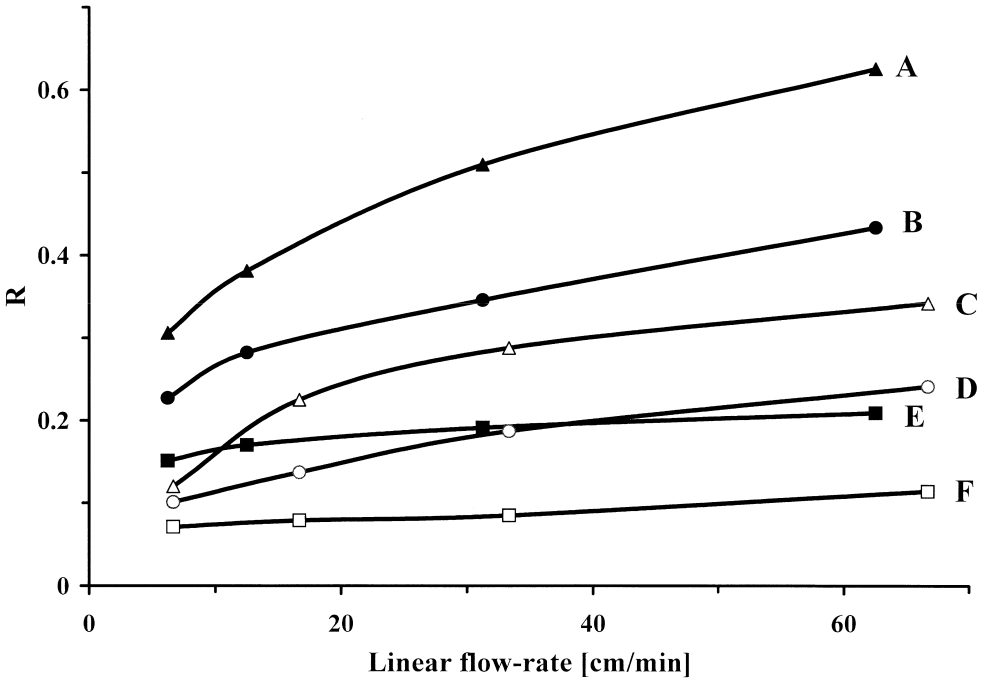

Fig. 6. The dependence of retention ratio R of the model silica gel particles on the linear flow-rate for two channel heights (80 and 150 μm). The shapes of the signs are used in the same way as in Fig. 5. The full signs denote $w=80$ μm, the empty signs denote $w=150$ μm. Curve A holds for 10-μm particles at $w=80$ μm, B for 5-μm particles at $w=80$ μm, C for 10-μm particles at $w=150$ μm, D for 5-μm particles at $w=150$ μm, E for 1.6-μm particles at $w=80$ μm, and F for 1.6-μm particles at $w=150$ μm. The concentrations of particles in model suspensions were 2 mg/ml, 8-μl volumes were injected. Water was used as the carrier liquid.

increases 100-times (from 0.67 to 66.67 cm/min) is 0.011, which is 22% of the difference $R_{exp}-R_{theor}$ (see Table 1). The difference between the retention behaviour of the silica particles in water and methanol could be explained by two facts.

(1) The value of the dielectric constant of methanol is lower than the value of water, thus the surfaces in methanol exhibit generally stronger electrostatic interactions.

(2) The lift forces are stronger in water than in methanol because of higher viscosity of water.

The electrostatic repulsion between the negatively charged glass channel wall and the negatively charged particles [24] could elevate the particle zone above the channel bottom. Thus, no particle can touch the channel accumulation wall, where there is expected the maximal concentration of the analyte in the ideal case of Brownian elution mode. Under the conditions when the lift forces or electrostatic repulsion become active, the Brownian mode changes in the focusing one. The particle–particle repulsion [25] is supposed to make the Brownian zone higher than expected based on its size and density, hence, to increase the mean layer thickness of the zone l. Both these effects cause the increase in R_{exp}.

In order to calculate the properties of analytes from retention data in Brownian elution mode it is necessary to eliminate hydrodynamic forces, particle–wall and particle–particle interactions. Some experiments with the aim to eliminate or weaken interfacial forces in water have been made [26–31].

4.2. Focusing elution mode

The increasing R_{exp} values with increasing flow-rates confirm that the 1.6-, 5- and 10-μm particles elute in focusing elution mode (see Figs. 5 and 6). This is also confirmed by the retention values presented in Tables 2 and 3. However, in some cases, the values R_{exp} are lower than R_{theor}. Especial-

ly, it is true for the 10-μm particles in methanol. The negative value of $R_{exp} - R_{theor}$ in Table 2 could be explained by lag effects. Based on the Faxen theory [34] on particle lag effect, the decrease of R_{exp} due to the lag effect was described [35] by Eq. (5)

$$R_L = R_{theor} - 2\alpha^2 \quad (5)$$

where R_L is the corrected retention ratio. For the 10-μm particle in methanol at $w = 80$ μm and the linear flow-rate 6.25 cm/min, the value R_{exp} equals 0.205. R_{theor} is 0.352 and Eq. (5) yields $R_L = 0.344$. It follows that Eq. (5) expresses only a part of the deviation from the theoretical value. It suggests that some additional effects are contributing to the particle lag.

We have found that suitable flow-rate conditions for the three particles studied and for the carrier liquids and the channels used here lie in the range of linear velocity: 6–67 cm/min. This range can be used for flow-rate programming in GFFF. Lower flow-rates would lead to long retention times and at higher flow-rates the particles of different diameters would be focused at too close positions and their resolution would be poor.

The flow-programming in the focusing elution mode mentioned here is substantially different from that one introduced by Giddings et al. [14] in sedimentation FFF for the hastened elution of late peaks, where the retention ratio was constant during the flow-programming. In the case of flow-programming in separations of silica gel particles in GFFF, the increasing flow of the carrier liquid induces higher hydrodynamic lift forces, which influences both resulting forces acting on particles and retention ratios. It means that the flow-programming in GFFF is in fact the field programming.

Furthermore, retention ratios can be influenced by changing carrier liquid density, as shown in Fig. 3 for methanol and water. The resulted retention ratio difference (R_{exp} in water $- R_{exp}$ in methanol) depends on the flow-rate and on the particle size, as shown in Fig. 7. The steeper slopes for the larger particles suggest that, with increasing flow-rate, the influence

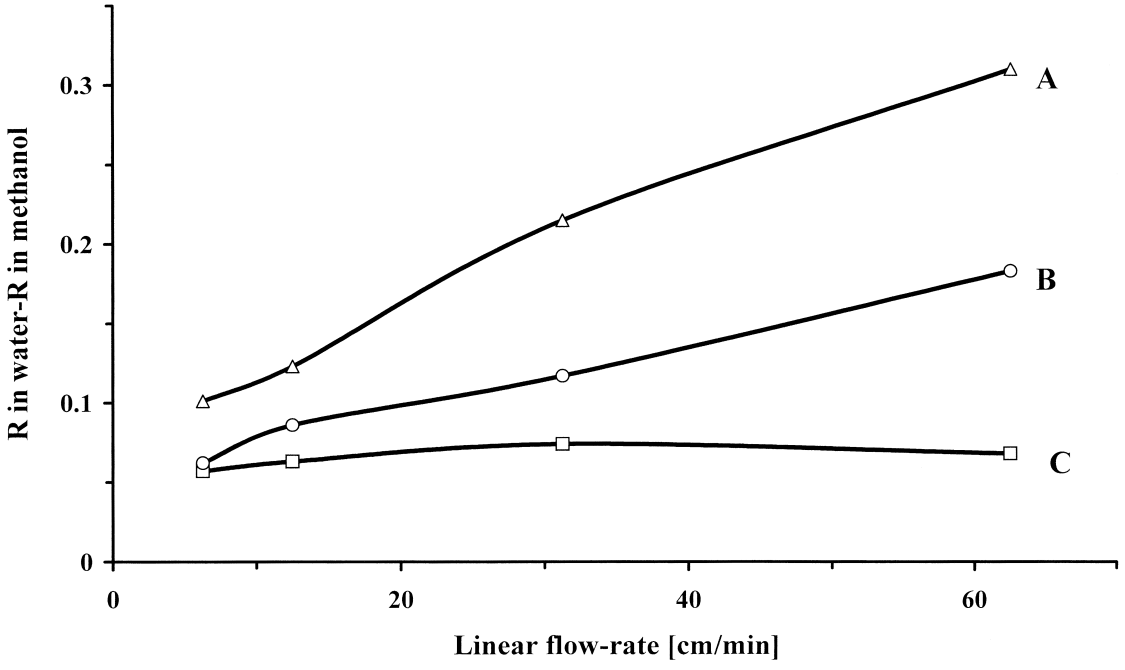

Fig. 7. The differences between the retention ratios of the model particles obtained in water as carrier liquid (*R* in water) and their retention ratios obtained in methanol (*R* in methanol) are plotted against linear flow-rate at the channel height 80 μm. The shapes of the signs are used in the same way as in Fig. 5. Curve A holds for 10-μm particles, B for 5-μm particles, and C for 1.6-μm particles. The concentrations of the particles in the model suspensions were 2 mg/ml and 8-μl volumes were injected.

of lift forces dominates the influence of carrier liquid density difference. The viscosity difference between water and methanol probably contributes to this phenomenon. Fig. 4 shows that even smaller carrier liquid density differences result in obviously changed values R_{exp}, which enables functioning of carrier liquid density gradients. The advantageous range of flow-rates for optimisation of the carrier liquid gradients is evident from Fig. 7 (from 60 cm/min to the limit given by peak broadening and resolution).

We have found and described the experimental conditions that can be used for force field programming in GFFF through modulating the linear velocity and density of the carrier liquid. Presently, gradient elutions as a tool for optimised separations are investigated. Preliminary results were already presented [36].

Acknowledgements

This work was supported by the Grant No. A4031805/1998 from the Grant Agency of Academy of Sciences of the Czech Republic. František Matulík is gratefully appreciated for technical support.

References

[1] J.C. Giddings, M.N. Myers, K.D. Caldwell, J.W. Pav, J. Chromatogr. 185 (1979) 261.
[2] J. Pazourek, E. Urbánková, J. Chmelík, J. Chromatogr. A 660 (1994) 113.
[3] J. Pazourek, K.-G. Wahlund, J. Chmelík, J. Microcol. Sep. 8 (1996) 331.
[4] P. Reschiglian, D. Melucci, G. Torsi, J. Chromatogr. A 740 (1996) 245.
[5] J. Pazourek, J. Chmelík, J. Microcol. Sep. 9 (1997) 611.
[6] J. Chmelík, A. Krumlová, J. Cáslavský, Chem. Papers 52 (1998) 360.
[7] J. Pazourek, J. Chmelík, Chromatographia 35 (1993) 591.
[8] R.E. Peterson II, M.N. Myers, J.C. Giddings, Sep. Sci. Technol. 19 (1984) 307.
[9] J.C. Giddings, M.N. Myers, Sep. Sci. Technol. 13 (1978) 637.
[10] P.J.P. Cardot, J. Gerota, M. Martin, J. Chromatogr. 568 (1991) 93.
[11] E. Urbánková, A. Vacek, N. Nováková, F. Matulík, J. Chmelík, J. Chromatogr. 583 (1992) 27.
[12] E. Urbánková, A. Vacek, J. Chmelík, J. Chromatogr. B 687 (1996) 449.
[13] F.J.F. Yang, M.N. Myers, J.C. Giddings, Anal. Chem. 46 (1974) 924.
[14] J.C. Giddings, K.D. Caldwell, J.F. Moellmer, T.H. Dickinson, M.N. Myers, M. Martin, Anal. Chem. 51 (1979) 30.
[15] J. Chmelík, J. Chromatogr. A 845 (1999) 285.
[16] K.D. Caldwell, T.T. Nguyen, J.C. Giddings, M.N. Myers, Sep. Sci. Technol. 14 (1979) 935.
[17] E. Urbánková, J. Chmelík, J. Liq. Chromatogr. 20 (1997) 637.
[18] J. Pazourek, J. Chmelík, J. Chromatogr. A 715 (1995) 259.
[19] J.C. Giddings, K.D. Caldwell, in: B.W. Rossiter, J.F. Hamilton (Eds.), Physical Methods of Chemistry, Vol. 3B, Wiley, New York, 1989, p. 867.
[20] J.C. Giddings, J. Chem. Educ. 50 (1973) 667.
[21] J.C. Giddings, Sep. Sci. Technol. 13 (1978) 241.
[22] H. Brenner, Adv. Chem. Eng. 4 (1966) 287.
[23] J. Pazourek, P. Filip, F. Matulík, J. Chmelík, Sep. Sci. Technol. 28 (1993) 859.
[24] P.S. Williams, Y. Xu, P. Reschiglian, J.C. Giddings, Anal. Chem. 69 (1997) 349.
[25] J.S. Jeon, M.E. Schimpf, A. Nyborg, Anal. Chem. 69 (1997) 3442.
[26] J. Plocek, P. Konečný, J. Chmelík, J. Chromatogr. B 656 (1994) 427.
[27] C. Bories, P.J.P. Cardot, V. Abramowski, C. Pous, A. Merino-Dugay, B. Baron, J. Chromatogr. 579 (1992) 143.
[28] V. Yue, R. Kowa, L. Neargarder, L. Bond, A. Muetterties, R. Parsons, Clin. Chem. 40 (1994) 1810.
[29] A. Bernard, B. Paulet, V. Colin, P.J.P. Cardot, Trends Anal. Chem. 14 (1995) 266.
[30] A. Athanasopoulou, G. Karaiskakis, A. Travlos, J. Liq. Chromatogr. Rel. Technol. 20 (1997) 2525.
[31] D. Meluci, G. Gianni, G. Torsi, A. Zattoni, P. Reschiglian, J. Liq. Chromatogr. Rel. Technol. 20 (1997) 2615.
[32] V.L. Kononenko, J.K. Shimkus, J. Chromatogr. 520 (1990) 271.
[33] P.S. Williams, T. Koch, J.C. Giddings, Chem. Eng. Commun. 111 (1992) 121.
[34] H. Faxen, Ark. Math. Astronom. Fys. 18 (1924) 1.
[35] M. Martin, J. Chromatogr. A 831 (1999) 73.
[36] J. Plocková, J. Chmelík, presented at the 13th Bratislava International Conference on Polymers, Bratislava, 4–9 July 1999, Poster No. II-9.